Preprints of the 2012 20th Mediterranean Conference on Control & Automation (MED), Barcelona, Spain, July 3-6, 2012

On Line Solar Irradiation Forecasting by Minimal Resource Allocating Networks

Lucio Ciabattoni, *Student Member, IEEE,* Massimo Grisostomi, Gianluca Ippoliti, Sauro Longhi, *Senior Member, IEEE,* and Emanuele Mainardi

***Abstract*— The paper describes an on-line prediction algorithm to estimate, over a determined time horizon, the solar irradiation of a specific site. The learning algorithm is based on a radial basis function network and combines the growing criterion and the pruning strategy of the minimal resource allocating network technique. An Extended Kalman Filter (EKF) is used to update all the parameters of the network. The on-line algorithm is able to avoid the initial training of the neural network. A comparison of the performance obtained by the MRAN EKF RBF Neural Network with respect to the standard RBF Neural Network is presented.**

I. INTRODUCTION

As concerns about climate change, rising fossil fuel prices, and energy security increase, there is growing interest around the world in renewable energy resources. Since most renewable energy sources are intermittent in nature, it is a challenging task to integrate a significant portion of renewable energy resources into the power grid infrastructure. Traditional electricity grid was designed to transmit and distribute electricity generated by large conventional power plants. The electricity flow mainly takes place in one direction from the centralized plants to consumers. In contrast to large power plants, renewable energy plants have less capacity, and are installed in a more distributed manner at different locations. The integration of distributed renewable energy generators has great impacts on the operation of the grid and calls for new grid infrastructure. Indeed, it is a main driver to develop the smart grid for infrastructure modernization, which monitors, protects, and optimizes the operation of its interconnected elements from end to end with a two-way flow of electricity and information to create an automated and distributed energy delivery network [1]. On the other hand, while renewable energy systems, such as photovoltaic and wind plants, have problems of controllability due to their intermittent output it becomes necessary to find a way to schedule power output in a deterministic manner. This problem has been deeply investigated in literature, in particular for what regards the forecasting and power scheduling from wind plant [21]. The prediction of solar yields is becoming more and more important, especially for countries where legislation encourages the deployment of solar power plants [27]. In Italy, where the installed photovoltaic (PV) power amounts is more than 8 GW, a proposal of law of 2009 incentived the scheduled power immission on the power line. This document, called "Terzo Conto Energia" (for further details see [29]), included 20% more incentives for PV plants with a correct hourly prediction of the power feeding the power line on the next day (with an error of less than 10%) for at least 300 days/year. Forecast informations on the expected solar power production are necessary for the management of electricity grids, for scheduling of conventional power plants, for decision making on the energy market, as described in [20], and moreover for energy home management [2]. In fact, today time of use tariffs, for domestic use of energy, penalize some periods of time with a higher price. Prosumers (customers and producers of energy at the same time), knowing their forecasted energy production profile can (re)arrange their processes to minimize costs, having great economic benefits.

Depending on the application and the corresponding time scale different approaches for modelling and forecasting solar irradiation may be appropriate. There have been a lot of researchers engaged in the modeling of solar irradiance. For example, the existing models include those called clear-day solar radiation, half-sine, Multi Layer Perceptron Network (MLP), Wavelet Decomposition Network (WD), Seasonal Auto Regressive Integrated Moving Average (SARIMA), WD-SARIMA, Support Vector Regression (see [22], [24], [25] and reference therein). However, the methods based on time series have not been efficient in all cases (most of them are efficient only for forecast up to 5-10 minutes [4], [19]) and contrarily they may yield to noised results. Indeed, Neural Networks (NNs) provide a generic black-box representation for implementing mappings. Radial Basis Function Networks (RBFNs) have been considered for the prediction considered in this paper and the system dynamics related to the irradiation have been taken into account through the RBFN input pattern that must be composed of a proper set of system input and output samples acquired in a finite set of past time instants [5]. These RBFs have been widely used for nonlinear system identification [6], [13] because they have the ability both to approximate complex nonlinear mappings directly from input-output data with a simple topological structure that avoid lengthy calculations [13] and to reveal how learning proceeds in an explicit manner [7]. These nets also avoid the non linear optimization techniques used in the learning algorithm of MLPs and the related problems of local minima [8]. Moreover in [9] has been proved that

This work was supported by the company Energy Resources spa

L. Ciabattoni, M. Grisostomi, G. Ippoliti, S. Longhi are with the Dipartimento di Ingegneria dell'Informazione, Università Politecnica delle Marche, 60131 Ancona, Italy, e-mail: {l.ciabattoni, m.grisostomi, gianluca.ippoliti, sauro.longhi}@univpm.it

E. Mainardi is with the company Energy Resources spa, via Ignazio Silone, 60035 Jesi (AN), Italy, e-mail: emanuele.mainardi@energyresources.it

978-1-4673-2529-5/12/$31.00 ©2012 IEEE

RBF networks do have the best approximation property with respect to MLPs and this significant result provides theoretical support for favoring RBF networks. The considered on-line learning algorithm is based on the Minimal Resource Allocating Network (MRAN) technique [7], [10], [11], that adds hidden neurons to the network based on the innovation of each new RBFN input pattern which arrives sequentially. As stated in [7], [11], to obtain a more parsimonious network topology a pruning strategy is introduced. This strategy detects and removes as learning progresses those hidden neurons which make little contribution to the network output. Pruning is necessary for the prediction of the irradiation changing dynamics because inactive hidden neurons could be present as the dynamics which caused their creation becomes nonexistent. If an observation has no novelty then the existing parameters of the network are adjusted by an Extended Kalman Filter (EKF) [11], [12]. The main advantage of this sequential learning method is that a large data set of irradiation measured, wheather forecast, temperature for a specific location is no longer required for the training of the Neural Network, drastically reducing setup time. A comparison of the performance obtained by the MRAN EKF RBF Neural Network with respect to the standard RBF Neural Network [28] is presented for a PV plant in the city of Jesi (AN) in Italy.

The paper is organized as follows. The on-line prediction algorithm is described in Section II and the performance of the considered NNs are discussed in Section III.

II. PREDICTION ALGORITHM

The following approach to implement a Minimal Resource Allocating Network (MRAN) is based on a sequential learning algorithm and an Extended Kalman Filter (EKF) [10]–[12]. In particular the sequential learning algorithm adds and removes neurons on-line to the network according to a given criterion [7], [10], [11] and an EKF is used to update the net parameters [12].

A. Radial Basis Function Neural Network

A RBFN with input pattern $\boldsymbol{x} \in \mathbb{R}^m$ and a scalar output $\hat{y} \in \mathbb{R}$ implements a mapping $f : \mathbb{R}^m \to \mathbb{R}$ according to

$$\hat{y} = f(\boldsymbol{x}) = \lambda_0 + \sum_{i=1}^{K} \lambda_i \phi\left(\|\boldsymbol{x} - \boldsymbol{c}_i\|\right) \tag{1}$$

where $\phi(\cdot)$ is a given function from $\mathbb{R}^+$ to $\mathbb{R}$, $\|\cdot\|$ denotes the Euclidean norm, λ_i, $i = 0, 1, \cdots, K$ are the weight parameters, $\boldsymbol{c}_i \in \mathbb{R}^m$, $i = 1, 2, \cdots, K$, are the radial basis function centers (called also units or neurons) and K is the number of centers [13]. The terms:

$$o_i = \lambda_i \phi\left(\|\boldsymbol{x} - \boldsymbol{c}_i\|\right), i = 1, \cdots, K \tag{2}$$

are called the hidden unit outputs.

In this paper the RBFN is used for the prediction of the output of a dynamical system and the system dynamics can be taken into account through the network input pattern $\boldsymbol{x}$, that must be composed of a proper set of system input and output samples acquired in a finite set of past time instants [5], i.e. $\boldsymbol{x} \in \mathbb{R}^{n_y+n_u}$ and it is defined as:

$$\boldsymbol{x}(n) = [y(n-1), \cdots, y(n-n_y), u(n-1), \cdots, u(n-n_u)]^T \tag{3}$$

where $n = 1, 2, \cdots$ are the time instants, $y(\cdot)$ and $u(\cdot)$ are the system output (the solar irradiation; see Section III) and input (whether forecast, the number of day of the year, the hour of the day; see Section III), respectively; n_y, n_u are the lags of the output and input, respectively.

Theoretical investigation and practical results show that the choice of the non-linearity $\phi(\cdot)$, a function of the distance d_i between the current input $\boldsymbol{x}$ and the centre $\boldsymbol{c}_i$, does not significantly influence the performance of the RBFN [13]. Therefore, the following gaussian function is considered:

$$\phi(d_i) = \exp\left(-d_i^2/\beta_i^2\right), \qquad i = 1, 2, \cdots, K \tag{4}$$

where $d_i = \|\boldsymbol{x} - \boldsymbol{c}_i\|$ and the real constant β_i is a scaling or "width" parameter [13].

B. Minimal Resource Allocating Network Algorithm

The learning process of MRAN involves allocation of new hidden units and a pruning strategy as well as adaptation of network parameters [10]–[12]. The network starts with no hidden units and as input-output data $(\boldsymbol{x}(\cdot), y(\cdot))$ are received, some of them are used to generate new hidden units based on a suitably defined growth criteria. In particular at each time instant n the following three conditions are evaluated to decide if the input $\boldsymbol{x}(n)$ should give rise to a new hidden unit:

$$\|e(n)\| = \|y(n) - f(\boldsymbol{x}(n))\| > E_1 \tag{5}$$

$$e_{rms}(n) = \sqrt{\sum_{j=n-(M-1)}^{n} \frac{e(j)^2}{M}} > E_2 \tag{6}$$

$$d(n) = \|\boldsymbol{x}(n) - \boldsymbol{c}_r(n)\| > E_3 \tag{7}$$

where $\boldsymbol{c}_r(n)$ is the centre of the hidden unit that is nearest to $\boldsymbol{x}(n)$ and M represents the number of past network outputs for calculating the output error $e_{rms}(n)$. The terms E_1, E_2 and E_3 are thresholds to be suitably selected. As stated in [7], [11], these three conditions evaluate the novelty in the data. If all the criteria of relations (5)–(7) are satisfied, a new hidden unit is added and the following parameters are associated with it:

$$\lambda_{K+1} = e(n) \tag{8}$$

$$\boldsymbol{c}_{K+1} = \boldsymbol{x}(n) \tag{9}$$

$$\beta_{K+1} = \alpha \|\boldsymbol{x}(n) - \boldsymbol{c}_r(n)\| \tag{10}$$

where α determines the overlap of the response of a hidden unit in the input space as specified in [11], [12]. If the observation $(\boldsymbol{x}(n), y(n))$ does not satisfy the criteria of relations (5)–(7), an EKF is used to update the following parameters of the network:

$$\boldsymbol{w} = \left[\lambda_0, \lambda_1, \boldsymbol{c}_1^T, \beta_1, \cdots, \lambda_N, \boldsymbol{c}_N^T, \beta_N\right]^T. \tag{11}$$

The update equation is given by:

$$\boldsymbol{w}(n) = \boldsymbol{w}(n-1) + \boldsymbol{k}(n)e(n) \tag{12}$$

where the gain vector $\boldsymbol{k}(n)$ is expressed by:

$$\boldsymbol{k}(n) = \boldsymbol{P}(n-1)\boldsymbol{a}(n)\left[r(n) + \boldsymbol{a}^T(n)\boldsymbol{P}(n-1)\boldsymbol{a}(n)\right]^{-1} \tag{13}$$

with $\boldsymbol{a}(n)$ the gradient vector of the function $f(\boldsymbol{x}(n))$ with respect to the parameter vector $\boldsymbol{w}(n-1)$ [11], [12], $r(n)$ is the variance of the measurement noise and $\boldsymbol{P}(n-1)$ is the error covariance matrix which is updated by:

$$\boldsymbol{P}(n) = \left[I - \boldsymbol{k}(n)\boldsymbol{a}^T(n)\right]\boldsymbol{P}(n-1) + \boldsymbol{Q}(n-1) \tag{14}$$

where $\boldsymbol{Q}(n-1)$ is introduced to avoid that the rapid convergence of the EKF algorithm prevents the model from adapting to future data [11], [12]. The $z \times z$ matrix $\boldsymbol{P}(n)$ is positive definite symmetric and z is the number of parameters to be adjusted. When a new hidden neuron is allocated, the dimension of $\boldsymbol{P}(n)$ increases to:

$$\boldsymbol{P}(n) = \begin{pmatrix} \boldsymbol{P}(n-1) & 0 \\ 0 & p_0 I_{z_1 \times z_1} \end{pmatrix} \tag{15}$$

where p_0 is an estimate of the uncertainty in the initial values assigned to the parameters and z_1 is the number of new parameters introduced by adding the new hidden neuron. As stated in [7], [11], to keep the RBF network in a minimal size a pruning strategy removes those hidden units that contribute little to the overall network output over a number of consecutive observations. To carry out this pruning strategy, for every observation $(\boldsymbol{x}(n), y(n))$ the hidden unit outputs are computed:

$$o_i(n) = \lambda_i \phi\left(\|\boldsymbol{x}(n) - \boldsymbol{c}_i\|\right), i = 1, \cdots, K \tag{16}$$

and normalized with respect to the highest output:

$$\overline{o}_i(n) = \frac{o_i(n)}{\max\{o_i(n)\}}, i = 1, \cdots, K. \tag{17}$$

The hidden units for which the normalized output (17) is less than a threshold δ for ξ consecutive observations are removed and the dimensionality of all the related matrices are adjusted to suit the reduced network [7], [11].

The EKF has been implemented with the assumption that $\boldsymbol{Q}(n) = I_{n,n}\sigma_\eta^2$ and $r(n) = \sigma_v^2$.

The MRAN prediction algorithm [7], [11] with the EKF, here called MRANEKF algorithm, is shown in Figure 1 and it is summarized as follow:

1. For each observation $(\boldsymbol{x}(n), y(n))$ do: compute the overall network output: $\hat{y}(n) = f(\boldsymbol{x}(n)) = \lambda_0 + \sum_{i=1}^{K} \lambda_i \phi\left(\|\boldsymbol{x}(n) - \boldsymbol{c}_i\|\right)$ where K is the number of hidden units;
2. Calculate the parameters required by the growth criterion:
   - $\|e(n)\| = \|y(n) - f(\boldsymbol{x}(n))\|$
   - $e_{rms}(n) = \sqrt{\sum_{j=n-(M-1)}^{n} \frac{e(j)^2}{M}}$

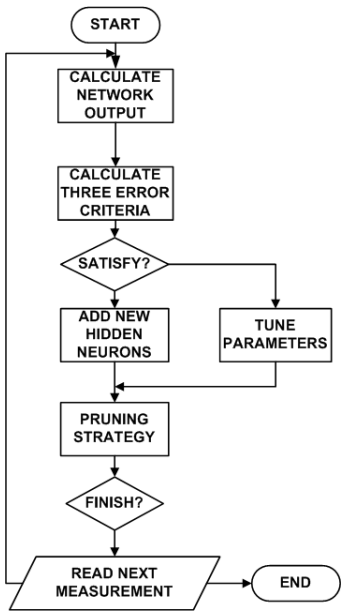

Fig. 1. Flow chart of the MRANEKF algorithm.

   - $d(n) = \|\boldsymbol{x}(n) - \boldsymbol{c}_r(n)\|$
3. Apply the criterion for adding a new hidden unit:
   if
   $\|e(n)\| > E_1$ **and** $e_{rms}(n) > E_2$ **and** $d(n) > E_3$ allocate a new hidden unit $K+1$ with:
   - $\lambda_{K+1} = e(n)$
   - $\boldsymbol{c}_{K+1} = \boldsymbol{x}(n)$
   - $\beta_{K+1} = \alpha\|\boldsymbol{x}(n) - \boldsymbol{c}_r(n)\|$

   else
   - tune the network parameters:
     $\boldsymbol{w}(n) = \boldsymbol{w}(n-1) + \boldsymbol{k}(n)e(n)$
   - update the error covariance matrix:
     $\boldsymbol{P}(n) = \left[I - \boldsymbol{k}(n)\boldsymbol{a}^T(n)\right]\boldsymbol{P}(n-1) + \boldsymbol{Q}(n-1)$

   end
4. Check the criterion to prune hidden units:
   - compute the hidden unit outputs:
     $o_i(n) = \lambda_i \phi\left(\|\boldsymbol{x}(n) - \boldsymbol{c}_i\|\right), i = 1, \cdots, K$
   - compute the normalized outputs:
     $\overline{o}_i(n) = \frac{o_i(n)}{\max\{o_i(n)\}}, i = 1, \cdots, K$
   - **if** $\overline{o}_i(\cdot) < \delta$ for ξ consecutive observations **than** prune the ith hidden unit and reduce the dimensionality of the related matrices

   end
5. $n = n + 1$ and **go** to step 1.

III. NEURAL NETWORK BASED SOLAR IRRADIATION FORECASTING

Tests are based on data acquired from January 2011 to December 2011 during PV plant standard working. In particular two different situations are considered. In the first one the proposed algorithm is tested without a pre-trained net; this situation can occur if the power production

has to be predicted on a plant without having previous data on panel orientation, tilting and irradiation on panel's plane. In the second situation it's used a pre-trained net with information about historical irradiation profile of clear sky days and cloudy days for the specified location, panel orientation and tilting. Those informations are taken directly from the website of PVGIS [30]; this is a common case, when no irradiation sensors are installed on the plant before the forecast begins. As measure of the performance of the proposed algorithm, the Root Mean Square of the Error $e(\cdot)$ (RMSE) and its Standard Deviation (SD) have been calculated. Only hours with daylight (irradiance greater than zero) are considered for the calculation of RMSE, night values with no irradiance are excluded from the evaluation. The set of experimental data is composed of 8000 pairs of input and output samples. Sampling time is $1\,\mathrm{h}$ and the data have been also normalized, between 0 and 1 in order to have the same range. Normalization is a widely used preprocessing method performed on data to distribute them evenly and to scale them into an acceptable range for the input neurons of the NN. This contributes to increase the NN ability to learn the association between inputs and outputs as well as to fasten significantly the calculations [15]–[17]. In particular the set of experimental data is given by the pairs $(\boldsymbol{x}(n), y(n))$, $n = 1, 2, \ldots$ where $\boldsymbol{x}(n)$ is composed by the whether forecast, the number of day of the year, the hour of the day, and $y(\cdot)$ is the solar irradiation. The lags of the output and input in Eq. (3) are $n_y = 1$, $n_u = 3$; different choices with an increment of these lags have been tested without significative improvements of the performance. The considered algorithm requires careful selection of the threshold parameters E_1, E_2, E_3 and of parameter M, as defined in Eqs. (5)–(7), which control the growth characteristics of the network; i.e. if small thresholds are chosen more units are added to the NN. The parameters δ and ξ control the pruning strategy (Eqs. (16) and (17)); it is important to take into account the system non stationarity to select these parameters. In other words, slowly dynamic variations imply a bigger δ and a smaller ξ. The parameters α, p_0, σ_v^2 and σ_η^2 related to the EKF algorithm used to update the network parameters of Eq. (11) are chosen by trial and error. In the considered experimental tests the numeric values of these parameters are selected, as: $E_1 = 0.01$, $E_2 = 0.02$, $E_3 = 0.4$, $M = 50$, $\delta = 0.0005$, $\xi = 2000$, $\alpha = 1.2$, $p_0 = 0.2$, $\sigma_v^2 = 0.001$, $\sigma_\eta^2 = 0.001$. Samples of the performed prediction tests are given in Figs. 2 through 6. In particular Fig. 2 shows the hidden neurons evolution history for the MRANEKF algorithm as it learns sequentially from data.

In this figure two data windows have been highlighted to compare the performance of the MRANEKF RBF NN in both the proposed situations (pre-trained and not pre-trained net) with respect to a classical RBF NN algorithm [28]. The first data window is relative to the initial learning period of the MRANEKF (January $17-19$), the second data window is relative to its "steady state" operation (June $12-16$). The training data set of the classical RBF Network is composed by 5000 pairs of inputs-output and it is relative to the last 20 days of each month of 2010 as described in [28]).

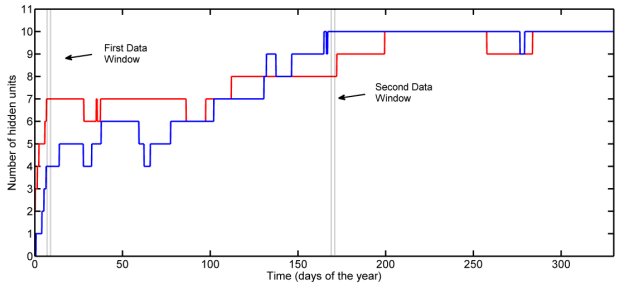

Fig. 2. Evolution of hidden neurons due to growing and pruning for the considered whole data set (Year 2011). The continuous red line is the pre-trained MRANEKF while the dashed blue line is the MRANEKF network without pre-training. The first data window is from January 17 to 19 ($144\,th$ to $216\,th$ sample); the second data window is from June 12 to 16 ($4032\,th$ to $4106\,th$ sample).

In Fig. 3, which refers to the first data window of Fig. 2, has been reported the solar irradiation predicted by the pre-trained MRANEKF network (continuous red line), by the MRANEKF network without pre-training (dashed blue line), by the classical RBF NN (dotted black line) and the measured solar irradiation (continuous green line).

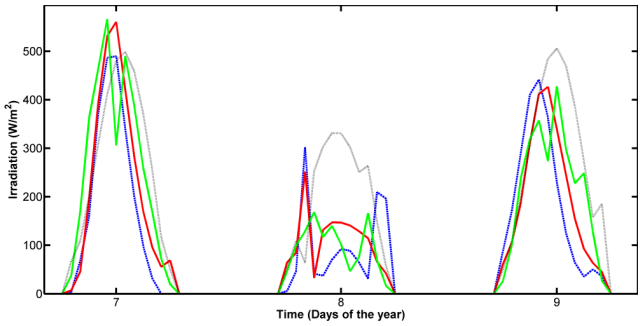

Fig. 3. First data window (January 17 - 19 of 2011). The continuous red line is the solar irradiation predicted by the pre-trained MRANEKF network, the dashed blue line is the solar irradiation predicted by the MRANEKF network without pre-training; the dotted black line is the solar irradiation predicted by the classical RBF NN and the continuous green line is the solar measured irradiation

The tests perform in the second data window have been reported in Fig. 4. In all the considered tests results indicate that the proposed MRAN algorithm realizes network with better prediction accuracy with respect to the classical RBF NN proposed in [28]. The RMSE and SD have been used to summarize the experimental results (see Table I). In this table have been also reported the tests performed on the whole data set (year 2011).

Another sample of the performed tests, when both considered MRANEKF RBF networks have a greater number of hidden units (the second considered data window), is shown in Fig. 4.

The whiteness test on the prediction errors (for both proposed MRANEKF networks) $e(\cdot)$ (residuals) has been used for network validation [18]. The whiteness of residuals

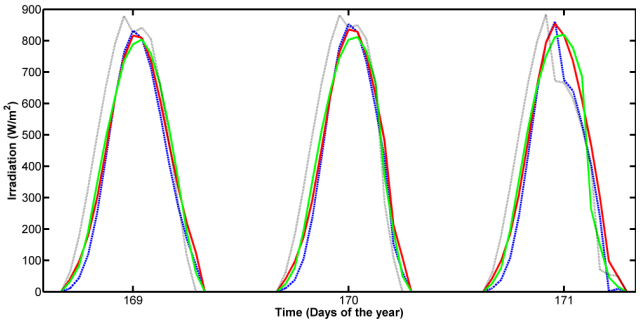

Fig. 4. Second data set (June $12-16$). The continuous red line is the solar irradiation predicted by the pre-trained MRANEKF network, the dashed blue line is the solar irradiation predicted by the MRANEKF network without pre-training; the dotted black line is the solar irradiation predicted by the classical RBF NN and the continuous green line is the solar measured irradiation

TABLE I

THE WHOLE DATA SET CONSIDERED IS RELATIVE TO THE YEAR 2011. THE DATA WINDOWS ARE ENLIGHTED IN FIG. 2.

	pre-trained MRANEKF	
DATA	RMSE	SD
Whole data set	$66.2W/m^2$	$61.2W/m^2$
First data window	$71.4W/m^2$	$70.2W/m^2$
Second data window	$50.9W/m^2$	$49.3W/m^2$

	not pre-trained MRANEKF	
Whole data set	$71.3W/m^2$	$69.2W/m^2$
First data window	$77.1W/m^2$	$75.8W/m^2$
Second data window	$56.5W/m^2$	$53.8W/m^2$

	classical RBF NN	
Whole data set	$75.1W/m^2$	$74.2W/m^2$
First data window	$81.2W/m^2$	$79.7W/m^2$
Second data window	$59.3W/m^2$	$57.1W/m^2$

is usually evaluated by computing the sample covariances

$$\hat{R}_e^N(\tau) = \frac{1}{N}\sum_{n=1}^{N} e(n)e(n+\tau) \tag{18}$$

with $\tau = 1, \ldots, P$.

If $e(\cdot)$ is a white-noise sequence, then the quantity

$$\zeta_{N,P} = \frac{N}{(\hat{R}_e^N(0))^2}\sum_{\tau=1}^{P}(\hat{R}_e^N(\tau))^2 \tag{19}$$

will have, asymptotically, a chi-square distribution $\chi^2(P)$ [18]. The independence between residuals can be verified by testing whether $\zeta_{N,P} < \chi^2_\alpha(P)$, the α level of the $\chi^2(P)$-distribution, for a significant choice of α. In Figs. 5 and 6 the sample covariance is reported for the whole data set (year 2011), have been considered the pre-trained and not pre-trained NNs. The whiteness test passes with $\alpha = 0.05$.

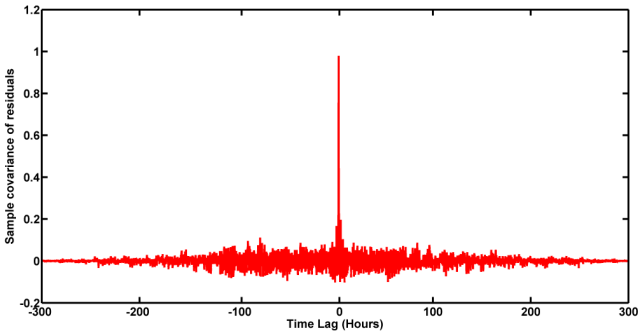

Fig. 5. Sample covariance of the residuals obtained by the prediction performed by the pre-trained MRANEKF network. The whiteness test passes with $\alpha = 0.05$.

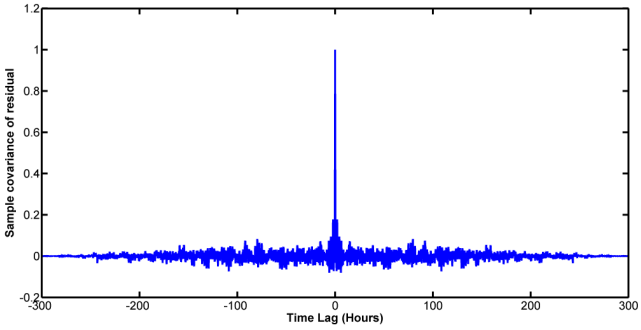

Fig. 6. Sample covariance of the residuals obtained by the prediction performed by the not pre-trained MRANEKF network. The whiteness test passes with $\alpha = 0.05$.

IV. CONCLUDING REMARKS

In this paper a Minimal Resource Allocating Network (MRAN) approach to derive hourly site-specific solar irradiance forecast from daily wheather forecasts has been analyzed. The considered algorithm is used to perform long range predictions. In particular, due to the aim of the work, the irradiation presented in the above tests is forecasted for 24 steps ahead predictions. The performance has been compared with a classical solution based on a RBF NN previously trained with a large data set. Since the proposed algorithm perform an on-line prediction of the solar irradiation it's possible to use it without having information on previous PV plant's irradiation. Two way of use of the MRANEKF algorithm have been proposed; with a pre-trained net based only on historical informations found on the web and with a not pre-trained net. The results indicate that both situations realizes network with better prediction accuracy with respect to a classical RBF algorithm.

REFERENCES

[1] Gungor, V.C.; Sahin, D.; Kocak, T.; Ergut, S.; Buccella, C.; Cecati, C.; Hancke, G.P.; , "Smart Grid Technologies: Communication Technologies and Standards," Industrial Informatics, IEEE Transactions on , vol.7, no.4, pp.529-539, Nov. 2011

[2] Palensky, P.; Dietrich, D.; , "Demand Side Management: Demand Response, Intelligent Energy Systems, and Smart Loads," Industrial Informatics, IEEE Transactions on , vol.7, no.3, pp.381-388, Aug. 2011

[3] Gungor, V. C., Lu, B., and Hancke, G. P., Opportunities and challenges of wireless sensor networks in smart grid, Industrial Electronics, IEEE Transactions on vol. 57, no. 10, pp. 35573564, Oct. 2010.
[4] Ben Salah, C. Ben Mabrouk, A. Ouali, M. , Wavelet autoregressive forecasting of climatic parameters for photovoltaic systems, Systems, Signals and Devices (SSD), 2011 8th International Multi-Conference on , 22-25 March 2011.
[5] K. J. Hunt, D. Sbarbaro, R. Zbikowski, P. J. Gawthrop, Neural networks for control systems - a survey, Automatica 28 (6) (1992) 1083–1112.
[6] M. Cavalletti, G. Ippoliti, S. Longhi, Lyapunov-based switching control using neural networks for a remotely operated vehicle, Int. J. of Contr. 80 (7) (2007) 1077–1091.
[7] L. Yingwei, N. Sundararajan, P. Saratchandran, Performance evaluation of a sequential minimal radial basis function (RBF) neural network learning algorithm, IEEE Trans. Neural Networks 9 (2) (1998) 308–318.
[8] M. Corradini, G. Ippoliti, S. Longhi, Neural networks based control of mobile robots: development and experimental validation, J. Robot. Syst. 20 (10) (2003) 587–600.
[9] T. Poggio, F. Girosi, Networks for approximation and learning, Proc. IEEE 78 (9) (1990) 1481–1497.
[10] J. Platt, A resource allocating network for function interpolation, Neural Computation 3 (1991) 213–225.
[11] N. Sundararajan, P. Saratchandran, Y. Li, Fully tuned radial basis function neural networks for flight control, Kluver Academic, London, Great Britain, 2002.
[12] V. Kadirkamanathan, M. Niranjan, A function estimation approach to sequential learning with neural network, Neural Computation 5 (1993) 954–975.
[13] S. Chen, C. F. N. Cowan, P. M. Grant, Orthogonal least squares learning algorithm for radial basis function networks, IEEE Trans. Neural Networks 2 (2) (1991) 302–309.
[14] B. Lennox, G. Montague, A. Frith, C. Gent, V. Bevan, Industrial application of neural networks an investigation, Journal of Process Control 11 (5) (2001) 497–507.
[15] J. Sola, J. Sevilla, Importance of input data normalization for the application of neural networks to complex industrial problems, IEEE Transactions on Nuclear Science 44 (3) (1997) 1464–1468.
[16] G. Chakraborty, B. Chakraborty, A novel normalization technique for unsupervised learning in ann, IEEE Transactions on Neural Networks 11 (1) (2000) 253–257.
[17] F. Aminian, M. Aminian, H. W. Collins, Analog fault diagnosis of actual circuits using neural networks, IEEE Transactions on Instrumentation and Measurement 51 (3) (2002) 544–550.
[18] L. Ljung, System identification, theory for the user, Information and System Sciences Series, Prentice Hall PTR, New Jersey, USA, 1999.
[19] Olavi Karner, ARIMA representation for daily solar irradiance and surface air temperature time series, Journal of Atmospheric and Solar-Terrestrial Physics, Volume 71, Issues 8-9, June 2009, Pages 841-847.
[20] Lange, M. ,"A mature market? The history of short term prediction services" *POW'WOW Best Practice Workshop, Delft, The Netherland*, 2006.
[21] Lange, M. , Focken, U. ,"Physical approach to short term wind power prediction" *New York: Springer*, 2005.
[22] Li, J. , Song, A.G. ,"Comparison of clear-day solar radiation model in Beijing to ASHRAE model" *Journal of Capital Normal University*, vol. 19, No. 1, pp 35-38, 1998.
[23] Ross, R.G., Flat-Plate Photovoltaic Array Design Optimization, Conference Record, 14th IEEE Photovoltaic Specialists Conference, San Diego, USA , pp. 1126-1132, 1980.
[24] Ren, M.J. , Wright, J.A. ,Adaptative diurnal prediction of ambient dry-bulb temperaature and solar radiation, HVAC and Research, Vol. 8, No. 4, 2002, pp. 383-401.
[25] Dorvlo, A.S.S. , Jervase, J.A., Ali, A.L. ,"Solar radiation estimation using artificial neural networks" *Applied Energy*,71: 307-319, 2002.
[26] Gonzlez-Longatt, F.M. ,"Model of Photovoltaic Module in Matlab" *II CIBELEC* ,2005.
[27] Lorenz, E., Hurka, J., Heinemann, D., Beyer, H.G., "Irradiance Forecasting for the Power Prediction of Grid-Connected Photovoltaic Systems," *IEEE Journal of Selected Topics in Applied Earth Observations and Remote Sensing*, vol.2, no.1, pp.2-10, March 2009.
[28] Ciabattoni, L., Ippoliti, G., Longhi, S., Cavalletti, M., Rocchetti, M., "Solar Irradiation Forecasting using RBF Networks for PV Systems with Storage" *IEEE ICIT Conference 2012*, Accepted for presentation, March 2012.
[29] (2010) GSE, Terzo Conto Energia, [Online] Available: http://www.gse.it/attivita/ ContoEnergiaF/PubblInf/GuideDM2010/Documents/GuidaTerzo Conto Energia (2).pdf, pages 6-7.
[30] (2011) Photovoltaic Geographical Information System, [Online] Available: http://re.jrc.ec.europa.eu/pvgis/